Plasmon Resonances within the Effective Susceptibility Concept: From Electrodynamics to Biological Applications

Valeri Lozovski

vlozovski@knu.ua

Educational Scientific Institute of High Technologies, Taras Shevchenko National University of Kyiv

Research Article

Keywords: nano system, plasmonic resonance, effective susceptibility, electrodynamic Green's function, antibacterial/antiviral effect

Posted Date: August 3rd, 2026

DOI: https://doi.org/10.21203/rs.3.rs-10226475/v1

Additional Declarations: No competing interests reported.

Plasmon Resonances within the Effective Susceptibility Concept: From Electrodynamics to Biological Applications

Valeri Lozovski
Educational Scientific Institute of High Technologies, Taras Shevchenko National University of Kyiv, 4-g Hlushkov ave., Kyiv 03022, Ukraine

Abstract

The description of resonance processes in nanoplasmonic structures within the framework of the electrodynamic Green's functions method and the concept of effective susceptibility is considered. This paper offers a unified perspective on plasmon resonance in spatially confined nanostructures and formulates the idea of dispersion relations in these systems. The local field enhancement effect is discussed as a resonant phenomenon. The concept of configurational resonances and its application in contemporary biology is also explored. Finally, the study examines surface plasmon resonance and its use in advanced sensor technology, with a specific focus on the *in situ* observation of biospecific interactions, such as those of an antigen-antibody type

Keywords: nano system; plasmonic resonance; effective susceptibility; electrodynamic Green's function; antibacterial/antiviral effect

Author's E-mail: vlozovski@knu.ua; ORCID: https://orcid.org/0000-0002-9142-0427

Introduction

Due to their unique optical properties, nanoplasmonic systems are widely used across various branches of contemporary science and technology [1]. These systems find fields of application as diverse as advanced optics [2,3], sensor technology [4,5], chemistry [6], and biomedicine [7]. One of the most significant characteristics of nanoplasmonic configurations is their resonant behavior, a feature that forms the bedrock of their widespread utility. For instance, they are instrumental in the development of optical filters [8] and integrated optical fiber-nanostructure devices [9]. Biosensors also commonly rely on surface plasmon resonance (SPR), with the application of SPR methods for chemical and biological sensing being particularly notable [4]. For example, a study [10] theoretically and experimentally investigated the possibility of in situ observation of biospecific antigen-antibody reactions using SPR on a gold surface coated with immunoglobulin molecules. All these applications share a common denominator: their efficiency relies inherently on the resonant properties of the underlying nanostructures. In this context, the use of nanoparticles to enhance the yield of photochemical processes is particularly noteworthy. Due to the local-field enhancement effect [11], the light intensity at the metal surface can dramatically increase, thereby boosting the efficiency of photochemical reactions by providing a higher concentration of photons per unit volume. This allows for the precise control of such reactions in sub-wavelength volumes, down to the nanometer scale. The concept of using a rough (nanostructured) metallic surface for heterogeneous catalysis to enhance chemical reactions was first proposed in [12] and experimentally implemented in [13], which demonstrated enhanced UV photodissociation of organometallic molecules at the surface of cadmium nanoparticles. Since then, numerous experiments have provided further proof of this concept [6]. In recent years, a large body of research has focused on utilizing nanosystems in medicine and biology, particularly for their antiviral and antimicrobial properties [14-16]. The primary mechanism behind the antiviral or antimicrobial action of these nanosystems is often attributed to chemical interactions between the nanostructures and the membrane of the virus or microbe [17]. However, as noted in various works (e.g., Refs. [17-19]), numerous experimental observations can be explained by nonchemical (field-based) mechanisms governing the nanosystem-pathogen interaction. These studies demonstrated that the local field enhancement effect creates domains with a strongly inhomogeneous local field. Consequently, ponderomotive forces arise. Acting on the dipole moments localized on the molecules that form the viral or bacterial envelope, these forces can distort the envelope's structure and even lead to its mechanical destruction. It is worth noting that all the effects and phenomena mentioned above can be modeled using a variety of approaches, which can be broadly divided into two major groups: numerical and analytical. Numerical methods, such as the discrete dipole approximation (DDA) [20] and the finite-difference time-domain (FDTD) method [21], are generally based on the direct solution of Maxwell's equations and are tailored to calculating the properties of specific systems. Consequently, any alteration to the system's parameters or geometry necessitates entirely new computational runs. Analytical methods, by contrast, offer greater universality as they allow one to analyze general trends in the properties of diverse systems. Prominent analytical approaches include Mie theory [22] and the Green's function method. This paper provides a mathematically grounded framework for describing plasmonic resonances using the electrodynamic Green's function formalism and the concept of effective susceptibility. In this work, we consider the features of nanoplasmonic systems from a general perspective, with a specific focus on their resonance properties. These properties are conveniently described using a unified mathematical approach, which is developed and discussed herein.

I. Ideas of plasmonic resonances (mathematical description)

The concept of plasmon resonance is conveniently described using the method of electrodynamic Green's functions. Below, we will briefly outline this idea. If the electrodynamic Green's function of the medium $G_{ij}(\mathbf{R},\mathbf{R}',\omega)$ is known, the electric field distribution, caused by a nano-object of volume V located within that medium is given by

$$E_i(\mathbf{R},\omega) = -i\omega\mu_0 \int_V d\mathbf{R}' G_{ij}(\mathbf{R},\mathbf{R}',\omega) J_j(\mathbf{R}',\omega) \ , \tag{1}$$

where $J_j(\mathbf{R},\omega)$ is the local current inside the nano-object. If the system under consideration is subjected to an external field, $E_i^{(0)}(\mathbf{R},\omega)$, the total (local) field at any point within the system will be the sum of the external field and the field caused by currents induced inside the nano-object

$$E_i(\mathbf{R},\omega) = E_i^{(0)}(\mathbf{R},\omega) - i\omega\mu_0 \int_V d\mathbf{R}' G_{ij}(\mathbf{R},\mathbf{R}',\omega) J_j(\mathbf{R}',\omega) . \quad (2)$$

Using the constitutive equation that connects the local current inside the nano-object and the local field,

$$J_j(\mathbf{R},\omega) = -i\omega\varepsilon_0 \chi_{jk}(\omega) E_k(\mathbf{R},\omega) , \quad (3)$$

one can obtain a self-consistent equation that connects the local and external fields (the Lippmann-Schwinger equation) [23]

$$E_i(\mathbf{R},\omega) = E_i^{(0)}(\mathbf{R},\omega) - k_0^2 \int_V d\mathbf{R}' G_{ij}(\mathbf{R},\mathbf{R}',\omega) \chi_{jk}(\omega) E_k(\mathbf{R}',\omega) , \quad (4)$$

where it was used that $\mu_0\varepsilon_0 = 1/c^2$ and introduced designation $k_0 = \omega/c$, with ω frequency and *c* velocity of light. This Fredholm integral equation of the second kind is the master equation in nano-optics. According to the existence and uniqueness theorem, the solution to Eq. (4) is guaranteed to be both existent and unique. While various approaches can solve the Lippmann-Schwinger equation, we will focus on a method that utilizes the concept of effective susceptibility [24].

a) *The effective susceptibility concept*

What does «effective susceptibility» mean? Let us suppose that the local current, $J_j(\mathbf{R},\omega)$, is connected to an external field, $E_k^{(0)}(\mathbf{R},\omega)$, through an expression similar to Eq. (3)

$$J_j(\mathbf{R},\omega) = -i\omega\varepsilon_0 \mathrm{X}_{jk}(\mathbf{R},\omega) E_k^{(0)}(\mathbf{R},\omega) . \quad (5)$$

Here, $\mathrm{X}_{jk}(\mathbf{R},\omega)$ is the effective susceptibility of the system under consideration. It is important to note that, unlike the material's polarizability, $\chi_{jk}(\omega)$, in constitutive equation [Eq. (3)], the effective susceptibility is a characteristic of the object itself, which is fabricated from that material. Consequently, the effective susceptibility obviously depends on the material's properties, as well as the object's dimensions and shape. The effective susceptibility for various nano-objects has been calculated, for example, in [24, 25]. In particular, the effective susceptibility of a nanoparticle located in a medium whose electrodynamic properties are described by a Green's function $G_{ij}(\mathbf{R},\mathbf{R}',\omega)$ has the form (Appendix A)

$$\mathrm{X}_{ji}(\mathbf{R},\omega) = \left[\left(\chi_{ji}(\omega)\right)^{-1} + k_0^2 \int_V d\mathbf{R}' G_{ij}(\mathbf{R},\mathbf{R}',\omega) \right]^{-1} , \quad (6)$$

where integration is over the volume of nanoparticle. Substituting Eq. (5) into Eq. (2) yields

$$E_i(\mathbf{R},\omega) = E_i^{(0)}(\mathbf{R},\omega) - k_0^2 \int_V d\mathbf{R}' G_{ij}(\mathbf{R},\mathbf{R}',\omega) \mathrm{X}_{jk}(\mathbf{R}',\omega) E_k^{(0)}(\mathbf{R}',\omega) . \quad (7)$$

This expression can be considered a solution to the Lippmann-Schwinger equation. Indeed, the primary advantage of the effective susceptibility method is that knowing the effective susceptibility – in any approximation – directly yields the solution to this equation. As a reminder, this solution is mathematically unique. Consequently, obtaining the effective susceptibility within a specific model or approximation practically equates to solving the Lippmann-Schwinger equation itself.

b) Formal description of plasmon resonance

Suppose a nano-object, characterized by an effective susceptibility $\mathrm{X}_{ij}(\mathbf{R},\omega)$, is located in a medium whose electrodynamical properties are described by the Green's function $G_{ij}(\mathbf{R},\mathbf{R}',\omega)$. This system is illuminated by an external monochromatic field $E_i^{(0)}(\mathbf{R},\omega) = E_i^{(0)} e^{i\mathbf{kR}} e^{-i\omega t}$. Let us define *plasmon resonance* as a non-zero response to an infinitesimally small external field, $E_i^{(0)} \to 0$. This means that if we assume $E_i^{(0)}(\mathbf{R},\omega) \to 0$ in Eq. (7), the solution for the total field *E* must be non-zero

$$\lim_{E_k^{(0)}\to 0}\int_V d\mathbf{R}' G_{ij}(\mathbf{R},\mathbf{R}',\omega)\mathrm{X}_{jk}(\mathbf{R}',\omega)E_k^{(0)}(\mathbf{R}',\omega) = A\ , \quad A\neq 0\ . \tag{8}$$

Since the effective susceptibility is the sole characteristic of the nano-object in this context, we can infer that the effective susceptibility must be infinitely large at least at some points within the volume of the nano-object

$$\mathrm{X}_{ij}(\mathbf{R}',\omega)\to\infty\ , \qquad \mathbf{R}'\in V\ . \tag{9}$$

This equation can be considered the local plasmon resonance condition. Taking into account Eq. (6), one can infer that this condition formally signifies

$$\mathrm{Re}\det\left[\left(\chi_{ji}(\omega)\right)^{-1} + k_0^2\int_V d\mathbf{R}' G_{ij}(\mathbf{R},\mathbf{R}',\omega)\right] = 0\ , \qquad \mathbf{R}\in V\ . \tag{10}$$

While Eqs. (8)–(10) are local in nature, plasmon resonance represents a global condition that characterizes the system as a whole. To clarify this concept, it should be noted that a system absorbs the energy of external radiation most efficiently under resonant conditions. To illustrate this behavior, let us examine the dissipative function of the system [26]

$$W = \left\langle \frac{1}{V}\int_V d\mathbf{R}\mathbf{J}(R,\omega)\mathbf{E}(R,\omega)\right\rangle = \frac{1}{4}\frac{1}{V}\int_V d\mathbf{R}\left(\mathbf{J}^*(\mathbf{R},\omega)\mathbf{E}(\mathbf{R},\omega) + \mathbf{J}(\mathbf{R},\omega)\mathbf{E}^*(\mathbf{R},\omega)\right)\ . \tag{11}$$

Suppose that the polarizability (the linear response to the local field, which is a characteristic of material) is given by $\chi_{jk}(\omega) = \chi(\omega)\delta_{jk}$. By taking into account Eq. (4) and the relationship between the local and external fields (which follows from comparing Eqs. (3) and (4)), one obtains the following for the absorption of linearly polarized monochromatic light

$$Q(\omega) = \frac{W}{\left|E_l^{(0)}\right|^2} = \frac{\omega\varepsilon_0}{2V}\,\mathrm{Im}\left[\left(\chi(\omega)\right)^{-1}\right]\int_V d\mathbf{R}\left|\mathrm{X}_{ij}(\mathbf{R},\omega)\right|^2\ . \tag{12}$$

First, let's consider a simple model for the nanoparticle – a nanoparticle shaped as a an ellipsoid of rotation. In this case, we can assume that the effective susceptibility of the nanoparticle is not dependent on the coordinate

$$\mathrm{X}_{ij}(\omega) = \chi(\omega)\frac{1}{1+4\pi\chi(\omega)L_i}\delta_{ij}\ , \tag{13}$$

where depolarization factors are determined according to

$$L_i = \frac{a_x a_y a_z}{2}\int_0^\infty \frac{ds}{(s+a_i^2)\sqrt{(s+a_x^2)(s+a_y^2)(s+a_z^2)}}\ , \tag{14}$$

with a_x, a_y, a_z semi-axes of ellipsoid. Let the external light be incident on the nanoparticle at an angle ϑ. The energy absorbed by the nanoparticle can then be calculated as a function of the frequency and the angle of incidence. This can be used to construct a «dispersion relation» for the nanoparticle, particularly if it's shaped as an ellipsoid of rotation [27]. The «mountain chain» of the surface of the dissipative function characterizes the conditions under which the dissipative function is maximized. Thus, the projection of these «mountain chains» onto the 'ω – k' plane provides the line of most effective light absorption by the particle. This line can be considered as dispersive curve of the system. The normalized dissipative function $Q(\omega)$ for a spherical nanoparticle made of a material with a resonance frequency of ω_0 obviously does not depend on the incidence angle and the projection of the surface is a straight line $\omega = \omega_r$, with ω_r resonance frequency of localized (at the nanoparticle) plasmon. It should be pointed out that this frequency does not coincide the

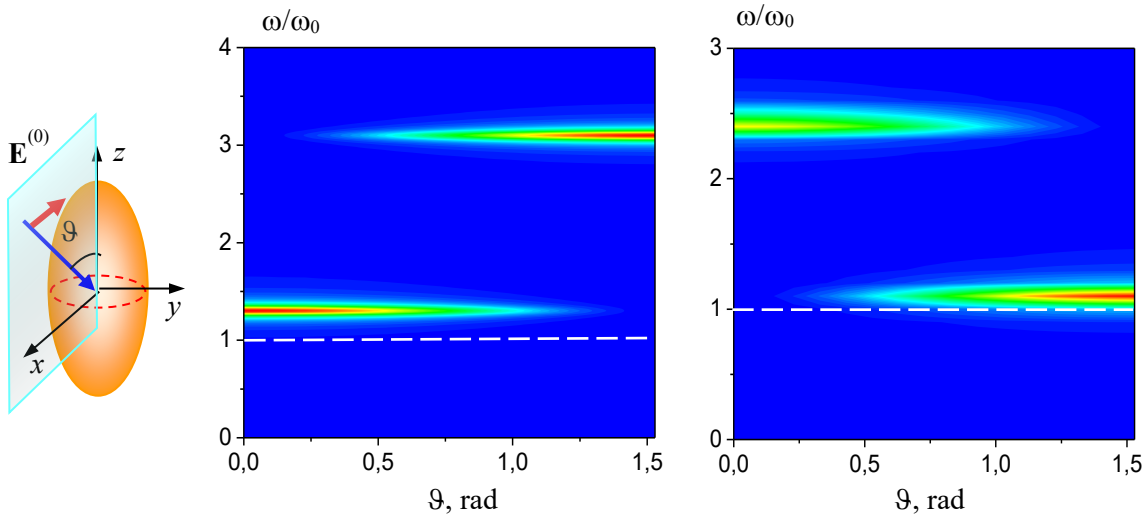

a b c

Fig.1. Dissipative functions Q of ellipsoidal particles. Calculations setup (a). The projection of the surface of Q for ellipsoidal nanoparticles shaped as oblate (b) and prolate (c) ellipsoids with eccentricity $a_z = 0.1a_x$ and $a_z = 10a_x$.

resonance frequency of material from which the nanoparticle is fabricated. Note that the resonance frequency ω_r corresponds to the dielectric constant of the material equaling −2, a condition known as the Fröhlich mode [28]. The behaviors of the dissipative functions for ellipsoidal nanoparticles – specifically, oblate (left) and prolate (right) ellipsoids with eccentricities $a_z = 0.1a_x$ and $a_z = 10a_x$, respectively – are shown in Fig.1. Unlike the spherical particle case, oblate and prolate particles are characterized by two resonant frequencies. This is a direct result of having two axes of symmetry.

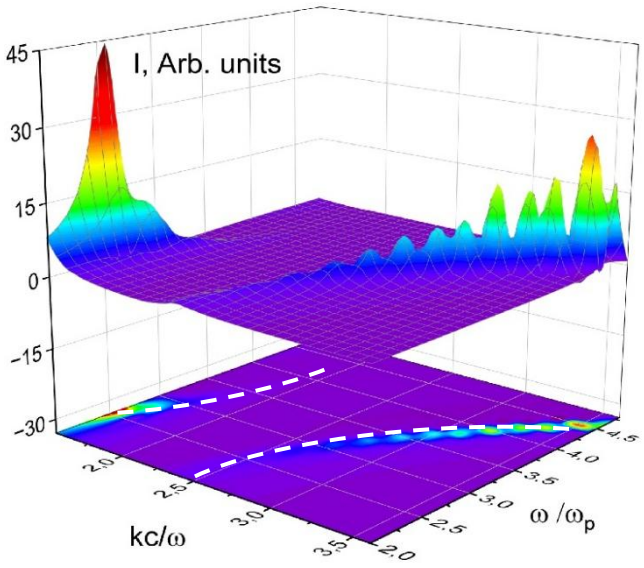

Fig.2. The absorption landscape for composite (the spheric Ag inclusions of radii r_p = 5 nm, f = 0.3 in dielectric matrix with ε_m = 2.1) calculated with Eq. (14); the map of this absorption landscape as a function of frequency (ω/ω_p) and wave vector (kc/ω) is the projection of landscape on the surface (ω/ω_p) - (kc/ω)

Similarly to ellipsoidal nanoparticles, the dissipative function for a cubic nanoparticle can be analyzed. However, in this case, a more general approach based on Eqs. (6) and (1) should be used. Theses calculation were provided in [27] and demonstrated six peaks in the absorption spectra. Similar results were obtained in the work [29], where the absorption spectra of a cubic Na nanoparticle were calculated by the Fuchs method [30], and by the DDA method [31]. The Fuchs method considers that the effective susceptibility of the particle is determined by the sum of the susceptibilities at the frequencies of the normal modes [30]. In both cases, complex spectra consisting of six peaks were obtained (Figs. 1,2 in [29]). The DDA method also yields additional structures that are qualitatively similar to those obtained by the effective susceptibility method. The difference from the spectra obtained by the Fuchs method is caused by the consideration of the cube's symmetry, as the Fuchs method uses several artificially defined vibration modes. The

difference in the details of the DDA result from the result obtained by the effective susceptibility method [27] is likely explained by a more accurate accounting of the local field's inhomogeneity inside the nanoparticle in the effective susceptibility method. Unfortunately, work [29] does not indicate the angle at which the test radiation was directed, making a direct comparison of the absorption spectra difficult. However, the general characteristics of these plasmon resonances, such as the number of resonances (six) and the presence of high-intensity main peaks, can still be compared. Based on the results above, we can define the dispersion relation for a nanosystem as the dependence of the energy characteristics of electromagnetic excitation on the spatial characteristics of the external influence that causes the excitation. This approach is rooted in finding solutions to a differential equation that describes an oscillatory process with an external driving force. If the frequency of this driving force matches the natural frequency of the oscillatory system, the system enters a resonance condition, where the oscillation amplitude can increase significantly (ideally, infinitely). Following this concept, the dissipative function of a nanocomposite was calculated in [26] using Eq. (12). The result of similar calculations for a nanocomposite consisting of spherical inclusions with a radius of r_p = 5nm and a filling factor of f = 0.3 in a dielectric matrix with ε_m = 2.1 is shown in Fig. 2. The dispersion curves are depicted as white dashed lines. A similar approach for studying resonance conditions in inhomogeneous sys-tems was reported in [32], where a system consisting of a gold film placed on glass with water as the ambient medium was considered. Some calculation results demonstr-ated in [32] are similar to those shown in Fig. 2. Namely, the projection line of the maximum of the normalized absorption surface onto the "energy–wave vector" plane (k_0–n_{eff}) corresponds to the dispersion curve of the excitation under study. This indicates that the efficiency of a nanoparticle's absorption of external radiation is determined by its effective susceptibility. Under resonance conditions, absorption becomes most efficient. On the other hand, light scattering is governed by the magnitude of the local field factor.

II. Local field factor and effect of local-field enhancing

Using Eqs.(3) and (5) it can be obtained the connection between the local $E_i(\mathbf{R},\omega)$ and external $E_k^{(0)}(\mathbf{R},\omega)$ fields

$$E_i(\mathbf{R},\omega) = L_{ik}(\mathbf{R},\omega)E_k^{(0)}(\mathbf{R},\omega) \ , \tag{15}$$

with so-called local-field factor

$$L_{ik}(\mathbf{R},\omega) = \left(\chi_{ji}(\omega)\right)^{-1} \mathrm{X}_{jk}(\mathbf{R},\omega) \ . \tag{16}$$

An analysis of these equations shows us that in the nano-systems described by the effective susceptibility $\mathrm{X}_{jk}(\mathbf{R},\omega)$ can be observed the domains of strong or weak local field. The emergence of domains with a strong local field is commonly referred to as the local-field enhancement effect [23, 33]. The formation of these domains, often called hot spots, is directly linked to the local maxima in the effective susceptibility tensor [see, Eqs. (15) and (16)], which in turn are related to its resonance properties. The local-field enhancement effect has been investigated extensively (see, for example, [34-39]). For instance, the local field distribution between two metal spheres was calculated in [39], where, particularly, the arising of a domain of a strong local field (hot spot) between the particles was demonstrated. This result illustrates a key characteristic of the local-field enhancement effect: the emergence of a hot spot in the gap between two nano-objects, and the enhancement of this effect as the gap size decreases. In [40], the local-field enhancement effect was studied within the framework of a generalized multiparticle Mie theory for metallic nanoparticles surrounded by small "satellite" clusters very close to their surface. It was established that the hot spot in such nano-systems is located in the gap between the particles. The enhancement factor in the case considered in [40] was approximately equal to180.

Another important characteristic of the local field enhancement effect is the strong spatial variation of the local field within a hot spot. The distribution of the local field, and thus the local field enhancement effect, can be of particular value in various applications. For example, Scanning Near-Field Optical Microscopy (SNOM) is based on measuring the local field distribution near the object under study [41]. Furthermore, to use surface plasmons in telecommunication technologies, it is necessary to control their propagation along a channel, which can be created in a flat photonic crystal [42] or in the form of a groove on a metal surface [43]. Numerous works have both calculated and measured local field distributions in two-dimensional surface plasmon channels (see, for example, [43–47]). Observing the spatial distribution

of a surface plasmon's evanescent field is challenging, as the wave is evanescent. Therefore, determining the local field inhomogeneity is often the only way to observe this distribution. A good example is the study in [44], which investigated the evanescent local field distribution of surface plasmon in planar waveguide systems. This work, in part, presented SNOM images of S-bends and Y-type splitters measured at different wavelengths. The results showed that similar planar structures can be successfully used as 2D waveguides for surface plasmons. The local field enhancement effect in a nanoparticle system is important to investigate from the perspectives of both fundamental knowledge and practical applications. For instance, this effect plays a significant role in the Tip-Enhanced Raman Scattering (TERS) phenomenon [48], where the local field enhancement near the probe tip greatly influences the effectiveness of Raman scattering. The distribution of the local field near two nanoparticles, caused by the local field enhancement effect, is important for analyzing the details of inter-nanoparticle interactions. In particular, it is crucial for studying the details of the antiviral action of nanoparticles. For example, a study [17] investigated the antiviral effect of gold nanoparticles. It was found that these nanoparticles exhibit a significant antiviral effect. In this work, the adenovirus and H1N1 influenza viruses were modeled as a spherical nanoparticle with a shell. Calculations of the local field distribution were performed using the pseudovacuum Green's function method [23] (Appendix B). Namely, it was considered a system with two nanoparticles: one small and one larger, with the larger nanoparticle treated as part of a "pseudovacuum." As the local field distribution, calculated using Eq. (16), shows, a domain of enhanced local field forms on the surface of the virus. This domain is characterized by strong inhomogeneity. According to reference [19], ponderomotive forces arise in this "hot spot" domain. These forces act on the virus envelope, causing damage that can lead to its destruction.

The local field enhancement effect in plasmonic solid-state nanostructures can significantly enhance the Brillouin light scattering (BLS) signal from thin magnetic films. This is achieved by placing a system of nano-objects on the film's surface. These can be simple metal nanoparticles of a specific shape and size, or more complex nanostructures, such as those investigated in studies [25, 49, 50].

Following Ref.[28], we can make the next speculation: When a plasmonic nano-system is located on a magnetic film, the field interacting with the magnons will consist of two parts. The first part is the initial field, $E_i^{(0)}(\mathbf{R},\omega)$, which exists inside the magnetic film without the nanoplasmonic cover. The second part is the field reradiated by the nanoplasmonic system, $E_i^{(rP)}(\mathbf{R},\omega)$. Thus,

$$E_i^{inc}(\mathbf{R},\omega) = E_i^{(0)}(\mathbf{R},\omega) + E_i^{(rP)}(\mathbf{R},\omega), \tag{17}$$

where

$$E_i^{(rP)}(\mathbf{R},\omega) = -k_0^2 \int_V d\mathbf{R}' G_{ij}^{(23)}(\mathbf{R},\mathbf{R}',\omega) \mathrm{X}_{jl}^{(P)}(\mathbf{R}',\omega) E_i^{(0)}(\mathbf{R},\omega), \tag{18}$$

with effective susceptibility $\mathrm{X}_{jl}^{(P)}(\mathbf{R}',\omega)$ of the nanoplasmonic cover, and $G_{ij}^{(23)}(\mathbf{R},\mathbf{R}',\omega)$ electrodynamic Green's function of three-layer system [51] – a substrate (layer 1), magnetic film (layer 2), and environment (layer 3). According to Ref.[25], the incoming field, $E_i^{inc}(\mathbf{R},\omega)$, induces a scattered field at a shifted frequency, $\bar{\omega} = \omega \pm \Omega$. This phenomenon is known as Brillouin Light Scattering (BLS), and the scattered field is represented by

$$E_i^{(BLS-I)}(\mathbf{R},\bar{\omega}) = -\bar{k}_0^2 \frac{\varepsilon_0}{4\pi} \int_{V_{\text{int}}} d\mathbf{R}' G_{ij}^{(32)}(\mathbf{R},\mathbf{R}',\bar{\omega}) \chi_{jl}(\mathbf{R}',\Omega) E_l^{(inc)}(\mathbf{R}',\omega), \tag{19}$$

with $\chi_{jl}(\mathbf{R}',\Omega)$ the susceptibility tensor in the first-order magneto-optical effects [52]. The presence of a nanoplasmonic system on the surface of the magnetic film introduces a second component to the scattered field, which is generated by scattering from this nanoplasmonic system. This second field is given by

$$E_i^{(BLS-II)}(\mathbf{R},\bar{\omega}) = -\bar{k}_0^2 \int_{V_{\text{int}}} d\mathbf{R}' G_{ij}^{(33)}(\mathbf{R},\mathbf{R}',\bar{\omega}) \mathrm{X}_{jl}^{(P)}(\mathbf{R}',\bar{\omega}) E_l^{(BLS-I)}(\mathbf{R}',\bar{\omega}). \tag{20}$$

The enhancement of the BLS signal is achieved when the effective susceptibility of the nanoplasmonic cover, $\mathrm{X}_{jl}^{(P)}(\mathbf{R}',\omega)$, reaches its maximum. This maximum is directly related to the local-field enhancement effect. When the nanostructures on the surface are positioned close enough to each other, the resonance condition corresponds to the

excitation of a surface plasmon localized at the nanosystem and propagating along the surface. An example of a calculation of the enhancement coefficient, K_{enh}, is shown in Fig. 3.

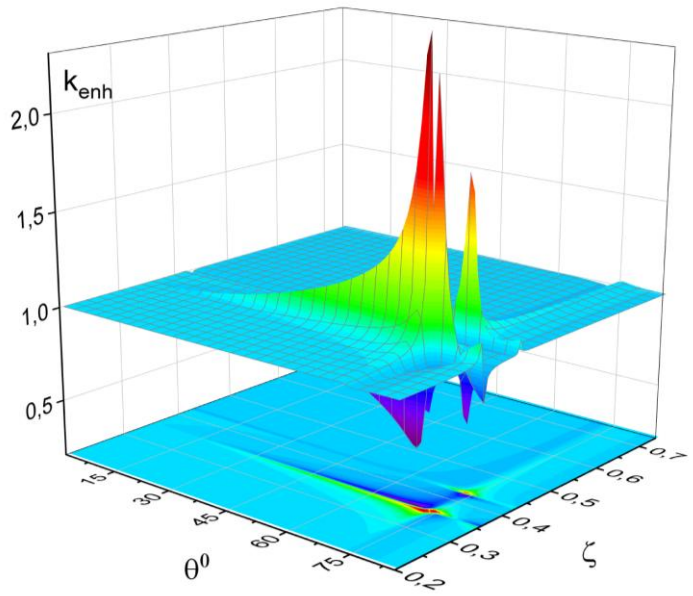

Fig.3. The image of enhancing coefficient of BLS for nanoplasmonic system on the surface of YIG film

$$K_{enh} = I_{np} / I_0 , \qquad (21)$$

where I_{np} and I_0 are the intensities of the BLS signal with and without nanosystem on the surface of magnetic film, respectively. Calculations were performed for the magneto-plasmonic system consisting of a 50 nm thick yttrium iron garnet (YIG) magnetic film with oblate silver nanoparticles on its surface. It was assumed that all nanoparticles are identical and have a 50 nm projection onto the film plane. The aspect ratio, defined as the height of the nanoparticle to its projection on the film, is denoted by ζ The surface concentration of nanoparticles is such that the average distance between them is 120–150 nm. The incident radiation is 400 nm p-polarized light with an angle of incidence of θ^0. The results show that a plasmonic resonance in the nanoplasmonic system with specific parameters (an ellipsoid eccentricity of approximately 0.4 and an incidence angle of about 45°) provides an enhancement coefficient of approximately 2.5. A small variation in the nanoparticle's shape (from ζ = 0.32 to 0.35) dramatically changes the effect, transforming the 2.2-fold enhancement into about of 2-fold attenuation.

III. Configurational resonances in nanoplasmonic systems

Consider a nanoplasmonic system composed of several nanoparticles, which are embedded in a medium whose electrodynamical properties are described by Green's function, $G_{ij}^{(0)}(\mathbf{R},\mathbf{R}',\omega)$. Let's single out one nanoparticle, say #1. As discussed in the Appendix B, we can then represent the other objects and their environment as a new environment described by the pseudovacuum Green's function, $G_{ij}^{(m)}(\mathbf{R},\mathbf{R}',\omega)$. The local field at any point inside the system can be defined by the expression

$$E_i(\mathbf{R},\omega) = E_i^{(0)}(\mathbf{R},\omega) - k_0^2 \int_V d\mathbf{R}' G_{ij}^{(m)}(\mathbf{R},\mathbf{R}',\omega) \mathrm{X}_{jk}^{(p)}(\mathbf{R}',\omega) E_k^{(0)}(\mathbf{R}',\omega) , \qquad (22)$$

where $\mathrm{X}_{jk}^{(p)}(\mathbf{R}',\omega)$ is the effective susceptibility of nano-object #1, described by the equation

$$\mathrm{X}_{ji}^{(p)}(\mathbf{R},\omega) = \left[\left(\mathrm{X}_{ji}^{(1)}(\omega) \right)^{-1} + k_0^2 \int_V d\mathbf{R}' G_{ij}^{(m)}(\mathbf{R},\mathbf{R}',\omega) \right]^{-1} . \qquad (23)$$

Here, $\mathrm{X}_{ji}^{(1)}(\omega)$ is the susceptibility of nanoparticle #1 in the medium, and the integration is performed over the volume of the nanoparticle. The plasmonic resonance in such a system, analogous to Eq.(10), is described by the equation

$$\mathrm{Re}\det \left[\left(\mathrm{X}_{ji}^{(1)}(\omega) \right)^{-1} + k_0^2 \int_V d\mathbf{R}' G_{ij}^{(m)}(\mathbf{R},\mathbf{R}',\omega) \right] = 0 . \qquad (24)$$

The solutions to this equation depend on both the properties of the individual nanoparticle #1 and the properties and mutual arrangement of all other nanoparticles in the system. This means the resonance is dependent on the system's configuration. Therefore, we are dealing with a *configurational resonance*.

The concept of configurational resonance was evidently first considered in reference [53]. That work studied resonant interactions between a SNOM probe and a surface using the point dipole approximation. These resonances were termed "configurational" because, for a given set of probe and surface characteristics, the system can be tuned to resonance by simply varying the distance between the probe and the surface, as well as the probe's coordinates in the plane where the dipoles are located. Essentially, this work formulated the main idea of using SNOM as a method for measuring the resonant condition between a probe and a surface. A similar problem was also considered in reference [54]. Configurational plasmon resonances can also be observed in nanocomposite systems. A large body of work on the optical properties of various nanocomposites has been, published recently (see, for example, [26], [55-59]). Specifically, reference [55] experimentally investigated plasmon resonances in a system of gold nanoparticles on a glass substrate, which were excited by normally incident light. It was shown that these plasmon resonances depend on the structure of the nanosystem (the period and shape of the nanoparticles) and the external environment. Configurational resonances in thin nanocomposite films with inclusions of different shapes distributed inhomogeneously along the film's thickness were considered in [26]. Using an approach based on calculating the dissipative function, it was shown that the resonant properties of these nanocomposite systems depend on their configuration. To illustrate the results from [26], the dissipative functions for nanocomposite thin Teflon films with gold nanoinclusions shaped as oblate ellipsoids of rotation were calculated. All calculations suggest that plasmon resonances are strongly dependent on the system's configuration. A large number of works studying the optical properties of various nanocomposites have been published recently. Reference [55] experimentally studied plasmon resonances in a system of gold nanoparticles on a glass substrate, which were excited by normally incident light. It was shown that the plasmon resonances in the system depend on the structure of the nanosystem (the period and shape of the nanoparticles) and the external environment.

The optical absorption by a semiconductor surface coated with metallic spheroidal nanoparticles was theoretically investigated in [56]. The methodology for calculating absorption in these structures was based on the concept of effective susceptibility within the electrodynamic Green's function formalism. Absorption spectra were computed for various nanoparticle shapes, surface concentrations, and angles of incident testing light. The results demonstrated configurational plasmon resonances, specifically, a resonant enhancement of absorption by nanoparticles of a particular shape and at a specific surface concentration. In the work [59], the optical properties of layered nanocomposite structures were investigated using the modified Maxwell-Garnett effective medium method. A crucial result from [59] is that the surface plasmon resonance exhibits a strong dependence on the particle distribution within the nanocomposite, consequently relying on the system's configuration.

IV. Plasmon resonances in biological systems

The effect of plasmonic resonance is widely used in modern biology, particularly in nanomedicine [60 – 62] and the sensorics of biological molecules [63–65]. Here we consider some applications of nanosystems in medicine and biology under plasmonic resonance conditions.

(*a*) *Interaction between bacteria and nanoparticles and nanostructured surface under plasmon resonance conditions*

Recently, a new branch of medicine, nanomedicine, has been actively developing [61, 62]. As we have already mentioned, the interaction of nanoparticles with viruses or bacteria leads to a decrease in their infectious activity. The reason for this antiviral/antibacterial effect is the formation of a strong local field domain (a hot spot) on the surface of the virus or bacteria shell. A hot spot is characterized by strong field inhomogeneity, which leads to the emergence of ponderomotive forces [19]. The action of ponderomotive forces can damage or even destroy the shell of a bio-object [17]. Let's consider the interaction of a spherical bacterium (for example, the opportunistic microorganism *Staphylococcus aureus*) with a metal nanoparticle (Fig. 4). For a simple model of interaction with a bacterium shaped like a sphere, ponderomotive forces are described by the expression

$$F_i(\mathbf{R}) = -k_o^2 \Xi_{jk}^{(v)}(\mathbf{R}) E_k^0(\mathbf{R}) \int_{V_v} d\mathbf{R}' \frac{\partial}{\partial x_j} G_{is}^{(m)}(\mathbf{R},\mathbf{R}') \Xi_{sl}^{(v)}(\mathbf{R}') E_l^{(0)}(\mathbf{R}') , \quad (26)$$

where $\Xi_{jk}^{(v)}(\mathbf{R})$ is the effective susceptibility of the system, $G_{is}^{(m)}(\mathbf{R},\mathbf{R}')$ is the electrodynamic pseudovacuum Green's function of the environment in which the bacterium is located (the bacterial suspension with gold nanoparticles), and $E_l^{(0)}(\mathbf{R}')$ is an external field. As this expression shows, under resonance conditions, when the effective susceptibility reaches its maximum values, the ponderomotive force can be significantly increased. This presents a potential additional tool for enhancing the antiviral/antibacterial action of nano-objects. The influence of surface plasmon resonance (SPR) on the antibacterial properties of a nanostructured surface can also be considered.

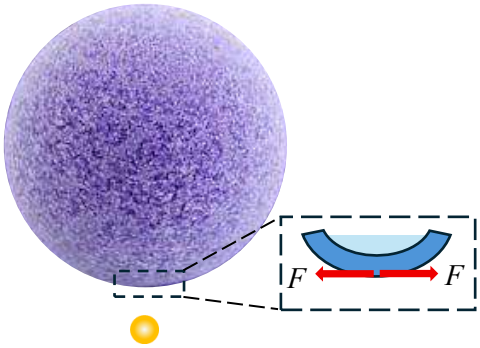

Fig.4. Cketch of the system bacterium-nanoparticle

The main idea behind such a study is to model the nanostructured surface as a flat surface covered by nanoparticles of different dimensions . In the experiments described in [66] a preparation of *Staphylococcus aureus* bacteria was circulated along the gold surface for 90 minutes. This can be viewed as the bacteria interacting with the nanoparticles that form the real surface of the gold film. As shown in [68], the adsorption potential between the nanoparticle and the surface increases approximately five-fold when the surface plasmon is excited along the surface. This means that the adsorption of bacteria onto the surface is more effective under plasmon resonance.

Additionally, in accordance with the previously presented ideas, the ponderomotive forces acting on the bacterial membrane increase under plasmon resonance conditions. The results of the experimental studies on the antibacterial action of a nanostructured surface under SPR conditions are presented in Fig. 5. The action of the nanostructured Au surface alone led to the destruction of 75% of the bacteria, but under SPR conditions, the destruction rate increased to

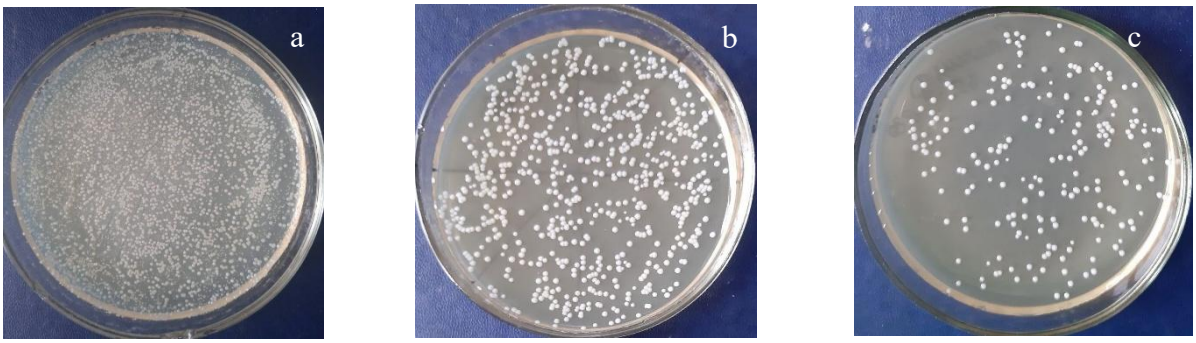

Fig.5. The influence of SPR for the bacteria *Staphylococcus aureus* . The control sample (a): bacteria form about 3000 colony forming units (CFU); the sample when bacterial suspension was pumped along Au surface without SPR (b): 740 CFU; the sample when bacterial suspension was pumped along Au surface under SPR (c): 220 CFU

93%. This result confirms the significant antimicrobial potential of nanostructured gold surfaces under surface plasmon excitation conditions.

(*b*) *Surface plasmon resonance in the sensorics of biomolecules*

In addition to localized plasmon resonance, there is another type associated with the propagation of a surface wave, which already was mentioned above. This wave is a coupled oscillation of the electromagnetic field and electron plasma near the metal-dielectric interface and is known as Surface Plasmon Resonance (SPR) [67-69]. SPR is a powerful optical technique used to study biomolecular interactions, particularly in sensing applications. It's a label-free method that allows real-time monitoring of binding events between biomolecules, providing information on kinetics and affinity. SPR-based biosensors are valuable tools in various fields, including biomedicine, drug discovery, and environmental

monitoring. To understand the idea of surface plasmon resonance, recall that a resonance condition, generally speaking, corresponds to a non-zero response (e.g., a local field) when the power of the source of the field is infinitesimally small. Let's consider a medium consisting of two half-spaces with a perfect planar interface. A field source $\mathbf{P}(\mathbf{R}',\omega)\to 0$ is located at the point $(\mathbf{r}',z')$, where $\mathbf{r}'$ is a 2D coordinate in a plane parallel to the interface at $z=z'$. The field at an arbitrary point $\mathbf{R}=(\mathbf{r},z)$ is given by

$$\mathbf{E}(\mathbf{R},\omega)=-\omega^2\mu_0\int_V d\mathbf{R}'\mathbf{G}^{(s)}(\mathbf{R},\mathbf{R}',\omega)\mathbf{P}(\mathbf{R}',\omega), \tag{27}$$

where $\mathbf{G}^{(s)}(\mathbf{R},\mathbf{R}',\omega)$ is the elecrtrodynamic Green's function of the medium. One can see that for the requirement $\mathbf{E}(\mathbf{R},\omega)\neq 0$, it is necessary for $\mathbf{G}^{(s)}(\mathbf{R},\mathbf{R}',\omega)\to\infty$. Because the system is homogeneous in the plane of the interface, we can perform a Fourier transformation on Eq. (27) to obtain

$$E_i(\mathbf{k},z,\omega)=-\omega^2\mu_0\int dz' G_{ij}(\mathbf{k},z,z',\omega)P_j(\mathbf{k},z',\omega). \tag{28}$$

Suppose that the field source is a point-like oscillating electric dipole $P_j(\mathbf{k},z'-z_0,\omega)=P_j(\mathbf{k},\omega)\delta(z'-z_0)$, then

$$E_i(\mathbf{k},z,\omega)=-\omega^2\mu_0 G_{ij}(\mathbf{k},z,z_0,\omega)P_j(\mathbf{k},z_0,\omega). \tag{29}$$

To obtain the condition for the resonant excitation of a surface wave, one needs to consider the explicit form of the Green's function. Let's consider a geometry where the wave vector **k** is directed along the X-axis of the Cartesian coordinates, and the XOZ plane is the incident plane [70]. Then, the explicit form of Green's function is

$$G_{ij}(\mathbf{k},z,z',\omega)=\begin{pmatrix}\frac{g_{11}}{P(\mathbf{k},\omega)} & 0 & \frac{g_{13}}{P(\mathbf{k},\omega)}\\ 0 & \frac{g_{22}}{S(\mathbf{k},\omega)} & 0\\ \frac{g_{31}}{P(\mathbf{k},\omega)} & 0 & \frac{g_{33}}{P(\mathbf{k},\omega)}\end{pmatrix}\times\begin{cases}e^{i\kappa_1(z-z')}, & z>0\\ e^{-i\kappa_2(z+z')}, & z<0\end{cases} \tag{30}$$

with $P(\mathbf{k},\omega)=\varepsilon_1\kappa_2+\varepsilon_2\kappa_1$, $S(\mathbf{k},\omega)=\kappa_1+\kappa_2$, $\kappa_1=\sqrt{\varepsilon_1 k_0^2-k^2}$, $\kappa_2=\sqrt{\varepsilon_2 k_0^2-k^2}$, $\mathbf{k}=(k,0,0)$. The interface coincides with the XOY plane. The upper half-space is characterized by dielectric constant ε_1 and the lower half-space by ε_2. The requirement that $G_{ij}(\mathbf{k},z,z_0,\omega)\to\infty$ means that the pole part of the Green's function must equal zero. Since the signs of the propagation constants κ_1 and κ_2 are defined, this requirement can be satisfied when $P(\mathbf{k},\omega)=0$. The equation

$$\varepsilon_1\sqrt{\varepsilon_2 k_0^2-k^2}+\varepsilon_2\sqrt{\varepsilon_1 k_0^2-k^2}=0 \tag{31}$$

can have a solution when the signs of ε_1 and ε_2 are different. The condition that the plasmonic excitation must be localized near the interface is $\sqrt{\varepsilon_2 k_0^2-k^2}\to i\sqrt{k^2-\varepsilon_2 k_0^2}$ and $\sqrt{\varepsilon_1 k_0^2-k^2}\to i\sqrt{k^2-\varepsilon_1 k_0^2}$. This implies that when the upper half-space is a vacuum or air ($\varepsilon_1=1$), the lower half-space should have $\varepsilon_2<0$. The surface plasmon can be excited by *p*-polarized light (with non-zero x- and z- components of the field in the geometry under consideration). The surface wave amplitude decreases approximately as $\exp(-\kappa_1 z)$ for $z>0$ and $\exp(-\kappa_1 z)$ for $z<0$. Equation (31) is the dispersion equation and a necessary condition for SPR. The dispersion relation of a surface plasmon depends strongly on the state of the interface. This fact forms the basis for using SPR in sensing applications. For example, let's consider the dispersion relation of a surface plasmon propagating along a "free" surface, represented by the red curve (labeled "1" in Fig. 6). When the surface is modified – for instance, by the adsorption of nanoparticles or molecules—the dispersion relation shifts to the black curve (labeled "2" in Fig. 6). This change means that the measured plasmon resonance curve, detected

by a sensor, will shift. This shift, of course, depends on the type, concentration, and distribution of the nano-objects or molecules on the surface, as well as the surrounding environment. Consequently, SPR is widely used in modern sensing [67-69, 71,72]. In particular, the SPR method is useful for observing in situ biospecific reactions, such as those between an antigen and an antibody. In [10], the concept of effective susceptibility was used to develop a method for determining the surface concentration of molecules (n_s) and the susceptibility components of a single molecule from SPR experiments. This approach is an alternative to the usual method of determining the effective layer thickness and refractive

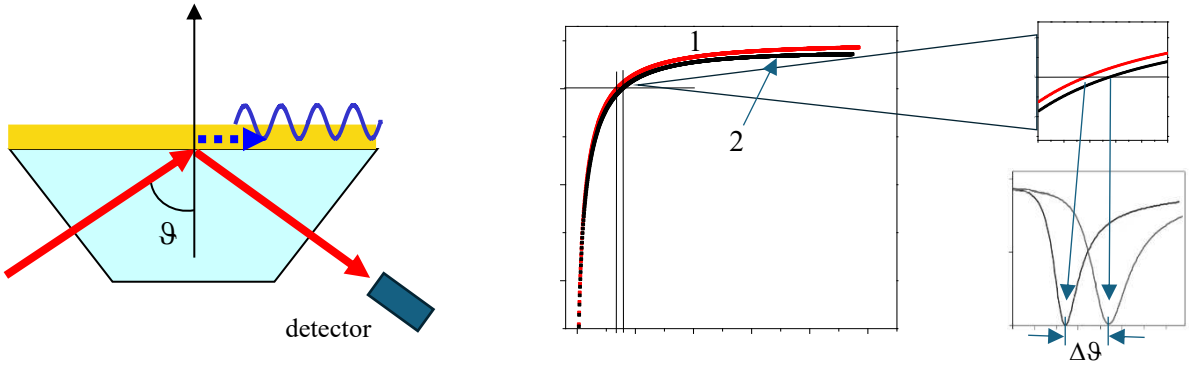

Fig.6. Sketch to idea of using the SPR for sensing

index. The paper [10] presents an expression for the effective susceptibility of a submonolayer of biomolecules covering the surface of a gold film in an SPR spectrometer

$$\mathrm{X}_{ij}^{(SC)}(\mathbf{k},z_a,\omega)=\left[\left(\tilde{\chi}_{ij}(\omega)\right)^{-1}+n_s G_{ji}(k,z_a,z_a,\omega)\right]^{-1}, \tag{32}$$

with $\tilde{\chi}_{ij}(\omega)$ the susceptibility of single biomolecules on the surface, $G_{ji}(k,z_a,z_a,\omega)$ electrodynamic Green's function of two half-spaces with the flat interface [Eq.(30)]. It was assumed that all molecules are located at the same distance (z_a) from the surface. By using Eq. (30), it was shown in [10] that the SPR response depends on both the shape and the orientation of the biomolecule relative to the metal surface along which the surface plasmon propagates.

Experimental data from the immunological reaction were used to calculate the surface molecular concentration and mass of the biomolecular coating. The biospecific interaction was considered between immunoglobulin (IgG) and anti-immunoglobulin (a-IgG) molecules. It was shown that it is possible to calculate nomograms for monolayers of a specified type of biomolecule (IgG) or biomolecular complex (IgG-a-IgG), accounting for their geometrical shape (or position) to determine the surface concentration of IgG molecules or IgG–anti-IgG complexes. Thus, using the SPR method, it is possible to estimate molecular adsorption directly in units of surface concentration n_s. Specifically, in [10], it was determined from a theoretical analysis using experimental data that the molecular concentration was $n_s \approx (1.1\pm 0.1)\cdot 10^{12}\,\mathrm{cm}^{-2}$. Therefore, the surface plasmon resonance effect allows for the *in situ* observation of biospecific reactions of the "antigen-antibody" type in real-time. This method can be used to determine the parameters of molecules on the surface, such as their concentration, the formation of biomolecular complexes, and their orientation relative to the surface plane.

Summary

In this work, we have analyzed how plasmon resonance gives rise to a variety of physical effects that are of significant interest from both fundamental and practical perspectives. From a theoretical standpoint, a comprehensive mathematical description of plasmon resonances in nanosystems is provided. Formally, for a homogeneous system where a Fourier transform is applicable, the plasmon resonance condition is determined by the pole contribution of the effective susceptibility (the linear response of the system to an external field), expressed as $\Xi_{jk}^{(v)}(\mathbf{k},\omega)=\left(N_{jk}(\mathbf{k},\omega)\right)\Big/P(\mathbf{k},\omega)$. In such homogeneous cases, the resonance condition reduces to the dispersion relation $\mathrm{Re}\,P(\mathbf{k},\omega)=0$. For inhomogeneous

systems, however, this standard approach becomes inadequate. Instead, we propose a novel method to determine plasmon resonance conditions by projecting the surface of the dissipative function in a three-dimensional space onto the (ω, **k**) plane. The projection of this "mountain range" – representing the regions of maximum absorption of external radiation – yields curves that couple the energy characteristics of plasmon excitation (frequency ω) with the spatial characteristics of the exciting radiation (wave vector **k**). This approach successfully yields the dispersion relations for inhomogeneous nanoplasmonic systems.

Utilizing the developed methodology, we evaluated several plasmonic effects driven by resonance conditions. In particular, we discussed that configurational resonance forms the foundation of scanning near-field optical microscopy and demonstrated how the local field enhancement effect can be utilized to suppress the infectious potential of viruses and bacteria. This antiviral and antibacterial action of nanoparticles or nanostructured surfaces is mediated by the emergence of ponderomotive forces, which lead to mechanical damage and the eventual destruction of the pathogen's envelope. Additionally, we addressed the application of plasmon resonances for the enhancement of Brillouin light scattering (BLS) signals in magnetoplasmonic systems. Finally, the conventional surface plasmon resonance (SPR) method for sensing applications was re-evaluated within the framework of the effective susceptibility concept. We highlighted the capability of this approach to advance the theory of the SPR sensing method and to determine critical molecular parameters, such as concentration and orientation relative to the surface plane.

Acknowledgments

The author thanks Dr. Taras Vasyliev and Dr. Nataliia Rybalchenko for valuable discussions.

Declaration

This research did not receive any funding

Appendix A. The effective susceptibility of nano-object

To calculate the effective susceptibility of the nanoparticle one can write the free energy of the nanoparticle placed into the medium electrodynamic properties of which are described by Green's function $G_{ij}(\mathbf{R},\mathbf{R}',\omega)$

$$F = \int_V d\mathbf{R}(U_{\text{int}} - P_i E_i) \ , \tag{1A}$$

where U_{int} is the internal energy of the particle, P_i is *i*-th component of polarization (density of electric dipole momentum) in the particle and E_i is the *i*-th component of local electric field at the particle. Integrations are over the volume of the particle. Suppose that the external electric field acts to the nanoparticle. Obviously this field induces the polarization inside the particle P_i . Let this field is less than intraparticle fields. In this case the addition to the internal energy of the particle caused by the dipole moment of the particle will be smaller than energy of the chemical bounds of the material. According to the ideas demonstrated in [73], one could represent the internal energies of the particle as the expansion in a Taylor series accurate within P^2

$$U_{\text{int}} = U_0 + \frac{1}{2\varepsilon_0}\lambda_{ij} P_i P_j + \ldots \tag{2A}$$

where tensor parameter λ_{ij} describes the linear polarizabilities of the particle. The first term in the series (U_0) is the internal energy of the particles (caused by interatomic bonds) which does not depend on the dipole moment P_i and can be omitted when the ground state of the system will be found.

To make it, one should write the exact form of the free energy and minimize it over induced dipole momentum. Then, one can write the free energy of the system in the form

$$F = \int_V d\mathbf{R}\left\{\frac{1}{2\varepsilon_0}\lambda_{ij} P_i(\mathbf{R}) P_j(\mathbf{R}) - P_i(\mathbf{R}) E_i(\mathbf{R})\right\}. \tag{3A}$$

The values $E_i(\mathbf{R})$ in this expression is the local field acting to the particle. The connection between the local field at arbitrary point of the system and the dipole moment density at the particle is [24]

$$E_j(\mathbf{R}) = E_j^{(0)}(\mathbf{R}) - \frac{k_0^2}{\varepsilon_0}\int_V d\mathbf{R}' G_{ji}(\mathbf{R},\mathbf{R}') P_i(\mathbf{R}') \,. \tag{4A}$$

The aim of the present calculations is the expression of the dipole momentum at the particle via the external field $E_j^{(0)}(\mathbf{R})$. Then, substitution of Eq.(4A) into Eq.(3A) gives

$$F = \int_V d\mathbf{R}\left\{\frac{1}{2\varepsilon_0}\lambda_{ij}P_i(\mathbf{R})P_j(\mathbf{R}) - P_i(\mathbf{R})\left[E_i^{\,0}(\mathbf{R}) - \frac{k_0^2}{2\varepsilon_0}\int_V d\mathbf{R}' G_{ij}(\mathbf{R},\mathbf{R}')P_j(\mathbf{R}')\right]\right\}. \tag{5A}$$

Note, the coefficient ½ in the third term of the integrand provides a one-time contribution from the self-action field. To obtain the equation which determines the dipole momentum in a ground state one needs to make a variation of the integral expression over the dipole momentum induced at the nano-object

$$\delta F(P_i(\mathbf{R})) = 0 \,. \tag{6A}$$

Then, one has the equation for finding the dipole moment at the particle introducing the linear response to the local field χ_{ji} $\left((\chi_{ji})^{-1} = \lambda_{ij}/2\right)$

$$\frac{1}{\varepsilon_0}(\chi_{ji})^{-1}P_j(\mathbf{R}) - E_i^{\,0}(\mathbf{R}) + \frac{k_0^2}{\varepsilon_0}\int_V d\mathbf{R}' G_{ij}(\mathbf{R}',\mathbf{R})P_j(\mathbf{R}) = 0 \tag{7A}$$

from which using the reciprocal theorem [$G_{ij}(\mathbf{R},\mathbf{R}')P_j^{\alpha}(\mathbf{R}') = G_{ij}(\mathbf{R},\mathbf{R}')P_j^{\alpha}(\mathbf{R})$] one obtains the connection between the local polarization in the nanoparticle and external field

$$\left[(\chi_{ij})^{-1} + k_0^2\int_V d\mathbf{R}' G_{ij}(\mathbf{R},\mathbf{R}')\right]P_j(\mathbf{R}) = \varepsilon_0 E_i^{\,0}(\mathbf{R}) \qquad \text{or} \qquad P_j(\mathbf{R}) = \varepsilon_0 \mathrm{X}_{ji}(\mathbf{R})E_i^{\,0}(\mathbf{R}) \tag{8A}$$

with effective susceptibility (the linear response to an external field).

$$\mathrm{X}_{ji}(\mathbf{R}) = \left[(\chi_{ij})^{-1} + k_0^2\int_V d\mathbf{R}' G_{ij}(\mathbf{R},\mathbf{R}')\right]^{-1} \,. \tag{9A}$$

Note, the same expression for effective susceptibility was obtained in [25] by direct solution of the Lippmann-Schwinger equation.

Appendix B. Pseudovacuum Green's function method

The idea of pseudovacuum Green's function was apparently first formulated in [23]. Consider a system consisting of the medium, electrodynamical properties of which are known and described by the photon propagator $G_{ij}^{(0)}(\mathbf{R},\mathbf{R}',\omega)$. Let in this medium the nanoparticle characterized by the effective susceptibility $\mathrm{X}_{kl}^{(p)}(\mathbf{R},\omega)$ are situated. Thus, the Green's function of the system can be calculated as

$$G_{ij}^{(m)}(\mathbf{R},\mathbf{R}',\omega) = G_{ij}^{(0)}(\mathbf{R},\mathbf{R}',\omega) - k_0^2\int_{V_p} d\mathbf{R}'' G_{ik}^{(0)}(\mathbf{R},\mathbf{R}'',\omega)\mathrm{X}_{kl}^{(p)}(\mathbf{R}'',\omega)G_{lj}^{(0)}(\mathbf{R}'',\mathbf{R}',\omega) \,, \tag{1B}$$

were integration is over the volume of nanoparticle. Indeed, when the source of the external field is point-like dipole

$$P_i^{(0)}(\mathbf{R}') = P_i^{(0)}\delta(\mathbf{R}' - \mathbf{R}_0) \,, \tag{2B}$$

then, the total (local) field in a point **R** will consist of the external field

$$E_i^{(0)}(\mathbf{R}) = -i\omega\int_{V_0} d\mathbf{R}' G_{ij}^{(0)}(\mathbf{R},\mathbf{R}')P_j^{(0)}(\mathbf{R}') = -i\omega G_{ij}^{(0)}(\mathbf{R},\mathbf{R}_0)P_j^{(0)} \,, \tag{3B}$$

and the field caused by the currents inside the particle, which are induced by the external field

$$J_k(\mathbf{R}) = -i\omega \int_{V_0} d\mathbf{R}' \mathrm{X}_{kl}^{(p)}(\mathbf{R}'',\omega) G_{lj}^{(0)}(\mathbf{R}'',\mathbf{R}',\omega) P_j^{(0)}(\mathbf{R}') = \\ = -i\omega \mathrm{X}_{kl}^{(p)}(\mathbf{R}'',\omega)(-i\omega) G_{lj}^{(0)}(\mathbf{R}'',\mathbf{R}_0,\omega) P_j^{(0)} \ . \tag{4B}$$

These currents, being integrated with the Green's function of the medium over the volume of the particle, form a field at point **R**

$$E_i^{(ind)}(\mathbf{R},\mathbf{R}',\omega) = -k_0^2 \int_{V_p} d\mathbf{R}'' G_{ik}^{(0)}(\mathbf{R},\mathbf{R}'',\omega) \mathrm{X}_{kl}^{(p)}(\mathbf{R}'',\omega)(-i\omega) G_{lj}^{(0)}(\mathbf{R}'',\mathbf{R}_0,\omega) P_j^{(0)} \ . \tag{5B}$$

Then the field at any point of the system consisting of the external environment and the nanoparticle, caused by the point dipole located at the point $\mathbf{R}_0$, will consist of the sum of the two fields

$$E_i(\mathbf{R}) = E_i^{(0)}(\mathbf{R}) + E_i^{(ind)}(\mathbf{R}) \ . \tag{6B}$$

Or, using Eqs.(3B) and (5B), one obtains

$$E_i(\mathbf{R}) = -i\omega G_{ij}^{(0)}(\mathbf{R},\mathbf{R}_0) P_j^{(0)} - \\ - k_0^2 \int_{V_p} d\mathbf{R}'' G_{ik}^{(0)}(\mathbf{R},\mathbf{R}'',\omega) \mathrm{X}_{kl}^{(p)}(\mathbf{R}'',\omega)(-i\omega) G_{lj}^{(0)}(\mathbf{R}'',\mathbf{R}_0,\omega) P_j^{(0)} \ . \tag{7B}$$

It is not difficult to see that such an expression for the field can be obtained if we assume that the point dipole is located

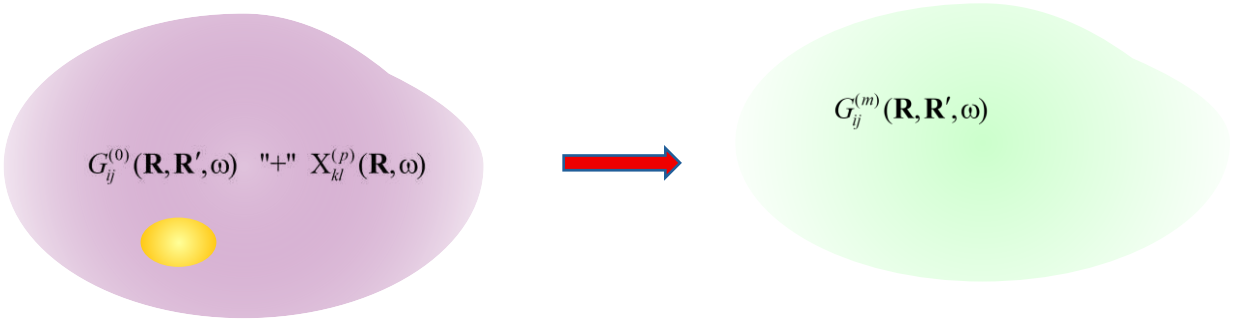

Fig.1B. To forming the new "pseudovacuum" medium consisting of a start medium characterized by Green's function $G_{ij}^{(0)}(\mathbf{R},\mathbf{R}',\omega)$ and nanoparticles with effective susceptibility $\mathrm{X}_{kl}^{(p)}(\mathbf{R},\omega)$.

in a new medium (pseudovacuum), the electrodynamic properties of which are described by the Green's function given by Eq.(1B) (see, Fig.1B). Namely

$$E_i(\mathbf{R}) = -i\omega G_{ij}^{(m)}(\mathbf{R},\mathbf{R}_0,\omega) P_j^{(0)} \ . \tag{8B}$$

The expression for the pseudovacuum Green's function leads from Eqs.(7B) and (8B)

$$G_{ij}^{(m)}(\mathbf{R},\mathbf{R}_0,\omega) = -i\omega G_{ij}^{(0)}(\mathbf{R},\mathbf{R}_0,\omega) \\ - k_0^2 \int_{V_p} d\mathbf{R}'' G_{ik}^{(0)}(\mathbf{R},\mathbf{R}'',\omega) \mathrm{X}_{kl}^{(p)}(\mathbf{R}'',\omega)(-i\omega) G_{lj}^{(0)}(\mathbf{R}'',\mathbf{R}_0,\omega) \ . \tag{9B}$$

References

[1]. Stockman Mark I (2011) Nanoplasmonics: past, present, and glimpse into future. Optics Express 19:22029-22106. https://doi.org/10.1364/OE.19.022029

[2]. Brongersma Mark L (2015) Introductory lecture: Nanoplasmonics, Faraday Discussions 178 (part 2). DOI: 10.1039/C5FD90020D

[3]. Bowei Dong, Yiming Ma, Zhihao Ren and Chengkuo Lee (2020) Recent progress in nanoplasmonics-based integrated optical micro/nano-systems. *J Phys D Appl Phys* 53: 213001. DOI: 10.1088/1361-6463/ab77db

[4]. Kurt Hasan, Pishva Parsa, Pehlivan Zeki Semih, Arsoy Elif Gül , Saleem Qandeel, Bayazıt Mustafa Kemal, Yüce Meral (2021) Nanoplasmonic biosensors: Theory, structure, design, and review of recent applications. Analytica Chimica Acta 1185:338842. DOI: https://doi.org/10.1016/j.aca.2021.338842

[5]. Yang Kang, Chen Yan, Sen Yan, Yang Wenxing (2023) Nanostructured surface plasmon resonance sensors: Toward narrow linewidths. Heliyon 9(6):e16598. DOI: https://doi.org/10.1016/j.heliyon.2023.e16598

[6]. Baffou Guillaume and Quidantn Romain (2014) Nanoplasmonics for chemistry. Chem Soc Rev 43:3898. DOI: 10.1039/c3cs60364d

[7]. Nanotechnology in Medicine and Biology (2021) Liu Huinan H, Shokuhfar Tolou, Ghosh Sougata. Elsevier. DOI: https://doi.org/10.1016/C2018-0-05429-8

[8]. Oh Jin-Woo, Choi Jongwan, and Kim Nakjoong (2009) Tunable color filter with surface plasmon resonance using organic photorefractive composite. Applied Optics 48(17): 3160-3164. DOI: https://doi.org/10.1364/AO.48.003160

[9]. Alba Calatayud-Sanchez, Angel Ortega-Gomez, Javier Barroso, Joseba Zubia, Fernando Benito-Lopez, Joel Villatoro, and Lourdes Basabe-Desmonts (2022) A method for the controllable fabrication of optical fiber-based localized surface plasmon resonance sensors. Sci Rep 12: 9566. DOI: https://doi.org/10.1038/s41598-022-13707-y

[10]. Chegel V, Chegel Yu, Guiver M D, Lopatynskyi A, Lopatynska O, Lozovski V (2008) 3D-quantification of biomolecular covers using surface plasmon-polariton resonance experiment. Sensors and Actuators B Chemical 134(1): 66–71. DOI: 10.1016/j.snb.2008.04.012

[11]. Ren S, Liu L-W, Li J-H, Hu S-Y, Ren Y, Wang Y, Xiu J-R (2018) Advances in the local field enhancement at nanoscale. Chinese Optics 11(1): 31-46. DOI: 10.3788/CO.20181101.0031

[12]. Nitzan A and Brus L E (1981) Theoretical model for enhanced photochemistry on rough surfaces. J Chem Phys 75: 2205-2214. DOI: https://doi.org/10.1063/1.442333

[13]. Chen C J and Osgood R M (1983) Direct Observation of the Local-Field-Enhanced Surface Photochemical Reactions. Phys Rev Lett 50: 1705. DOI: https://doi.org/10.1103/PhysRevLett.50.1705

[14]. Milovanovic Marija, Arsenijevic Aleksandar, Milovanovic Jelena, Kanjevac Tatjana, Arsenijevic Nebojsa (2017) Nanoparticles in Antiviral Therapy. Antimicrob Nanoarchitecton 383–410. DOI: 10.1016/B978-0-323-52733-0.00014-8

[15]. Ali Muhammad Aanish, Rehman Nagina, Park Tae Joo, and Basit Muhammad Abdul (2023) Antiviral role of nanomaterials: a material scientist's perspective. RSC Adv 13: 47-79. DOI: 10.1039/D2RA06410C

[16]. Mehran Alavi, Pragathi Kamarasu, David Julian McClements, Matthew D. Moore, Metal and metal oxide-based antiviral nanoparticles: Properties, mechanisms of action, and applications, Advances in Colloid and Interface Science, 306, 102726 (2022), https://doi.org/10.1016/j.cis.2022.102726

[17]. Chaika M, Zahorodnya S, Naumenko K, Pankivska Yu, Povnitsa O, Mukha Yu, Vityuk N, Dorovskih A, Lokshyn M, Lysenko V, Lozovski V, and Rusinchuk N (2022) Virus deformation or destruction: sizedependence of antiviral and virucidal activities of gold nanoparticles. Adv Nat Sci: Nanosci Nanotechnol 13: 035008. DOI: https://doi.org/10.1088/2043-6262/ac879a

[18]. Valeri Z Lozovski, Volodymyr S Lysenko and Natalia M Rusinchuk, Near-field interaction explains features of antiviral action of non-functionalized nanoparticles, Adv. Nat. Sci.: Nanosci. Nanotechnol., 11, 015014 (2020), https://doi.org/10.1088/2043-6254/ab7910

[19]. Lozovski Valeri, Lysenko Volodymyr and Rusinchuk Natalia (2022) Ponderomotive forces in the system of two nanoparticles. Sci Rep 12:17768. DOI: https://doi.org/10.1038/s41598-022-22510-8

[20]. Barchiesi D, Kessentini S, Guillot N, Chapelle M Lamy de la, and Grosges T (2013) Localized surface plasmon resonance in arrays of nano-gold cylinders: inverse problem and propagation of uncertainties. Opt Express 21(2): 2245-2262. DOI: https://doi.org/10.1364/OE.21.002245

[21]. Calà Lesina Antonino, Vaccari Alessandro, Berini Pierre, and Ramunno Lora (2015) On the convergence and accuracy of the FDTD method for nanoplasmonics. Opt Express 23:10481-10497.

DOI: https://doi.org/10.1364/OE.23.010481

[22]. Wriedt Thomas, Mie Theory: A Review Chapter 2 (2012) Hergert W and Wriedt T (eds.) The Mie Theory Springer Series in 53 Optical Sciences 169: 53-71 Springer-Verlag Berlin Heidelberg. DOI: 10.1007/978-3-642-28738-1_2

[23]. Keller Ole (1996) Local Fields in the Electrodynamics of Mesoscopic Media. Phys Rep 268: 85-262. DOI: https://doi.org/10.1016/0370-1573(95)00059-3

[24]. Lozovski V (2010) The Effective Susceptibility Concept in the Electrodynamics of Nano-Systems. J Comput Theor Nanosci 7: 2077-2093. DOI:10.1166/jctn.2010.1588

[25]. Lozovski Valeri and Chumak Andrii V (2024) Plasmon-enhanced Brillouin light scattering spectroscopy for magnetic systems: Theoretical model. Phys Rev B 110: 184419. DOI: 10.1103/PhysRevB.110.184419

[26]. Lozovski Valeri Z, Razumova Margarita A (2018) Optical response of thin nanocomposite films with transverse inhomogeneity. Physica B: Condensed Matter 545:420–432. DOI: https://doi.org/10.1016/j.physb.2018.06.041

[27]. Lozovski V and Tsykhonya A (2007) Dispersion Properties of Nano-Scale Systems. Internat J of Theor Phys, Group Theory, and Nonlinear Optics 12(3): 31-51.

[28]. Barnes William L (2016) Particle plasmons: Why shape matters. Am J of Phys 84(8): 593-601. DOI: 10.1119/1.4948402

[29]. Ruppin R (1996) Plasmon frequencies of cube shaped metal clusters. Z Phys D 36: 69-71. DOI: https://doi.org/10.1007/BF01437423

[30]. Fuchs R (1975) Theory of the optical properties of ionic crystal cubes. Phys Rev B 11: 1732 –1740 . DOI: https://doi.org/10.1103/PhysRevB.11.1732

[31]. Yurkin Maxim A (2023) Discrete dipole approximation, Chapt.9 in Light, Plasmonics and Particles., Ed. by Mengüç M Pinar and Francoeur Mathieu: 167-198. Elsevier. DOI: https://doi.org/10.1016/B978-0-323-99901-4.00020-2

[32]. Sarkar Mitradeep, Besbes Mondher, Moreau Julien, Bryche1 Jean-François, Olivéro Aurore, Barbillon Grégory, Coutrot Anne-Lise, Bartenlian Bernard, Canva Michael (2015) Hybrid plasmonic mode by resonant coupling of localized plasmons to propagating plasmons in a Kretschmann configuration. ACS Photonics 2 (2): 237-245. DOI: 10.1021/ph500351b.

[33]. Dolgaleva Ksenia and Boyd R obert W (2012) Local-field effects in nanostructured photonic materials. Adv in Optics and Photonics 4(1): 1-77. DOI: https://doi.org/10.1364/AOP.4.000001

[34]. Lereu Aude, Passian Ali, Dumas Philippe (2012) Near field optical microscopy: A brief review. Internat J of Nanotechnol 9(9): 3-7. DOI: 10.1504/IJNT.2012.045353

[35]. Zhou Jun, Zhang Jian-Shuo, Xian Guo-Yu, Qi Qi, Gu Shang-Zhi, Shen Cheng-Min, Cheng Zhao-Hua, He Sheng-Tai, and Yang Hai-Tao (2019) Synthesis and surface plasmon resonance of Au‑ZnO Janus nanostructures. Chinese Phys B 28: 083301. DOI: 10.1088/1674-1056/28/8/083301

[36]. Demchenko Hanna O, Rusinchuk Natalia (2019) Evaluation of the Efficiency of Interparticle Interactions in Nanosystems. J of Nanotechnology 2:1-8. DOI: 10.1155/2019/4270454

[37]. Hsu Liyi, Baida Fadi I, Ndao Abdoulaye (2021) Local field enhancement using a photonic-plasmonic nanostructure, Opt Express 29(2): 1102-1108. Doi: 10.1364/OE.415956.

[38]. Chung Taerin, Lee Seung-Yeol, Song Eui-Young, Chun Honggu, Lee Byoungho (2011) Plasmonic Nanostructures for Nano-Scale Bio-Sensing. Sensors 11: 10907-10929. DOI: 10.3390/s111110907

[39]. Tian Shuo, Wang Junqiao, Sun Shuai, He Mengyue, Mao Yu, Gao Ya, Ding Pei (2023) Strong field enhancement and hot spot manipulation based on anapole state in Si disk-ring metasurface. Results in Physics 49:106485. DOI: https://doi.org/10.1016/j.rinp.2023.106485

[40]. Pellegrini G, Mattei G, Bello V, Mazzoldi P (2008) Local-field enhancement in metallic nanoplanets. Materials Sci and Engineering B 149: 247–250. DOI: 10.1016/j.mseb.2007.09.060

[41]. Bozhevolnyi Sergey I, Smolyaninov Igor I, and Zayats Anatoly V (1995) Near-field microscopy of surface-plasmon polaritons: Localization and internal interface imaging. Phys Rev B 51:17 916-17930.
DOI: https://doi.org/10.1103/PhysRevB.51.17916

[42]. Boltasseva Alexandra, Søndergaard Thomas, Nikolajsen Thomas, Leosson Kristjan, Bozhevolnyi Sergey I, and Hvam Jørn M (2005) Propagation of long-range surface plasmon polaritons in photonic crystals. J Opt Soc Am B 22(9): 2027- 2038. DOI: https://doi.org/10.1364/JOSAB.22.002027

[43]. Bozhevolnyi Sergey I, Volkov Valentyn S, Devaux Eloïse, and Ebbesen Thomas W (2005) Channel Plasmon-Polariton Guiding by Subwavelength Metal Grooves. Phys Rev Lett 95: 046802. DOI: 10.1103/PhysRevLett.95.046802

[44]. Volkov Valentyn S, Bozhevolnyi Sergey I (2006) Bend loss for channel plasmon polaritons. Appl Phys Lett 89: 143108. DOI: 10.1063/1.2358953

[45]. Ung T P L, Quélin X, Laverdant J, Fulcrand R, Hermier J-P, and Buil S (2021) Localization of plasmon modes in a 2D photonic nanostructure with a controlled disorder. Opt Express 29 (13): 20776.
DOI: https://doi.org/10.1364/OE.424970

[46]. Takeuchi K and Yamamoto N (2011) Visualization of surface plasmon polariton waves in two-dimensional plasmonic crystal by cathodoluminescence. Opt Express, 19(13): 12365-12374.
DOI: https://doi.org/10.1364/OE.19.012365

[47]. Lozovski Valeri Z, Beermann Jonas, and Bozhevolnyi Sergey I (2007) Modeling of second-harmonic scanning optical microscopy of molecular quasi-one-dimensional aggregates. Phys Rev B 75: 045438.
DOI: 10.1103/PhysRevB.75.045438

[48]. Itoh Tamitake, Procházka Marek, Dong Zhen-Chao, Ji Wei, Yamamoto Yuko S, Zhang Yao, Ozaki Yukihiro (2023) Toward a New Era of SERS and TERS at the Nanometer Scale: From Fundamentals to Innovative Applications. Chem Rev 123: 1552−1634. DOI: https://doi.org/10.1021/acs.chemrev.2c00316

[49]. Demydenko Yurii, Vasiliev Taras, Levchenko Khrystyna O, Chumak Andrii V, and Lozovski Valeri (2025) Plasmon-enhanced Brillouin light scattering spectroscopy for magnetic systems. II. Numerical simulations. Phys Rev B 111: 014405. DOI: 10.1103/PhysRevB.111.014405

[50]. Wojewoda Ondřej, Hrtoň Martin, Dhankhar Meena, Krčma Jakub, Davídková Kristýna, Klíma Jan, Holobrádek Jakub, Ligmajer Filip, Šikola Tomáš, Urbánek Michal (2023) Phase-resolved optical characterization of nanoscale spin waves. Appl Phys Lett 122: 202405. DOI: https://doi.org/10.1063/5.0151338

[51]. Bach M L, Akjouj A and Dobrzynski L (1992) Response functions in layered dielectric media. Surf Sci Rep 16: 95-131. DOI: https://doi.org/10.1016/0167-5729(92)90010-9

[52]. Cochran J F and Dutcher J R (1988) Calculation of the Intensity of Light Scattered From Magnons in Thin Films. J Magn Magn Mater 73: 299-310.

[53]. Keller Ole, Xiao Mufei, Bozhevolnyi Sergey (1993) Configurational resonances in optical near-field microscopy: a rigorous point-dipole approach. Surf Sci 280: 217-230. DOI: https://doi.org/10.1016/0039-6028(93)90370-Y

[54]. Cai-zhang Wu, Xiao-bo Mao, Zhen-fang Xu, and Hu-nian Ye (2007) Configuration resonance in scattering scanning near-field optical microscopy. Optoelectron Lett 3: 289-293. DOI**:** 10.1007/s11801-007-6091-6

[55]. Thackray Benjamin D, Kravets Vasyl G, Schedin Fred, Auton Gregory, Thomas Philip A, and Grigorenko Alexander N (2014) Narrow Collective Plasmon Resonances in Nanostructure Arrays Observed at Normal Light Incidence for Simplified Sensing in Asymmetric Air and Water Environments. ACS Photonics 1:1116−1126.
DOI: Dx.doi.org/10.1021/ph5002186

[56]. Lozovski V Z, Lienau C, Tarasov G G, Vasyliev T A, Zhuchenko Z Ya (2019) Configurational resonances in absorption of metal nanoparticles seeded onto a semiconductor surface. Results in Physics 12: 1197-1201.
DOI: https://doi.org/10.1016/j.rinp.2018.12.091

[57]. Kravets V G, Kabashin A V, Barnes W L, Grigorenko A N (2018) Plasmonic Surface Lattice Resonances: A Review of Properties and Applications. Chem Rev*,* 118(12): 5912-5951. DOI: 10.1021/acs.chemrev.8b00243

[58]. Nishijima Yoshiaki, Rosa Lorenzo, and Juodkazis Saulius (2012) Surface plasmon resonances in periodic and random patterns of gold nano-disks for broadband light harvesting. Opt Express 20(10): 11466-11477.
DOI: https://doi.org/10.1364/OE.20.011466

[59]. Czajkowski K M, Świtlik D, Langhammer C, *et al.* (2018) Effective Optical Properties of Inhomogeneously Distributed Nanoobjects in Strong Field Gradients of Nanoplasmonic Sensors. Plasmonics 13: 2423–2434.
DOI: https://doi.org/10.1007/s11468-018-0769-4

[60]. Murthy Shashi K (2007) Nanoparticles in modern medicine: State of the art and future challenges, Int J Nanomedicine, 2(2): 129–141.

[61]. Mageed Heidi Abdel, Abuelezz Nermeen, Radwan Rasha, Mohamed Saleh Ahmed (2021) Nanoparticles in Nanomedicine: A Comprehensive Updated Review on Current Status, Challenges and Emerging Opportunities. J of Microencapsulation 38(3):1-61. DOI: 10.1080/02652048.2021.1942275

[62]. Eker Furkan, Akdaşçi Emir, Duman Hatice, Bechelany Mikhael, and Karav Sercan (2024) Gold Nanoparticles in Nanomedicine: Unique Properties and Therapeutic Potential. Nanomaterials 14(22): 1854. DOI: https://doi.org/10.3390/nano14221854

[63]. Špringer Tomáš, Bocková Markéta, Slabý Jiří, Sohrabi Foozieh, Čapková Magdalena, Homola Jiří (2025) Surface plasmon resonance biosensors and their medical applications. Biosensors and Bioelectronics 278: 117308. DOI: https://doi.org/10.1016/j.bios.2025.117308

[64]. Sepúlveda B, Calle A, Lechuga L M, and Armelles G (2006) Highly sensitive detection of biomolecules with the magneto-optic surface-plasmon-resonance sensor. Optics Lett 31(8): 1085-1087. DOI: https://doi.org/10.1364/OL.31.001085

[65]. Butt Muhammad A (2025) Surface Plasmon Resonance-Based Biodetection Systems: Principles, Progress and Applications – A Comprehensive Review. Biosensors 15(1): 35. DOI: https://doi.org/10.3390/bios15010035

[66]. Lozovski Valeri, Rybalchenko Nataliia, Petrik Iryna, Kryvokhyzha Kostiantyn, Vasiljev Anatoliy, Vasyliev Taras (2025) Surface Plasmon Resonance Influence on the Antibacterial Effect of a Nanostructured Gold Surface. e-J Surf Sci Nanotechnol 23: 160–167. DOI: 10.1380/ejssnt.2025-024

[67]. Englebienne Patrick, Van Hoonacker Anne, Verhas Michel (2003) Surface plasmon resonance: principles, methods and applications in biomedical sciences. J of Spectroscopy 17: 255–273. DOI: https://doi.org/10.1155/2003/372913

[68]. Shpacovitch Victoria (2012) Application of Surface Plasmon Resonance (SPR) for the Detection of Single Viruses and Single Biological Nano-objects. J Bacteriol Parasitol 3(7): 1000e110. DOI: 10.4172/2155-9597.1000e110

[69]. Shpacovitch Victoria, Hergenröder Roland (2020) Surface Plasmon Resonance (SPR)-Based Biosensors as Instruments with High Versatility and Sensitivity. Sensors (Basel) 20(11): 3010 DOI: 10.3390/s20113010

[70] Maradudin A A and Mills D L (1975) Scattering and absorption of electromagnetic radiation by a semi-infinite medium in the presence of surface roughness. Phys Rev B 11: 1392-1415. DOI: https://doi.org/10.1103/PhysRevB.11.1392

[71]. Homola Jiri, Yee Sinclair S, Gauglitz Günter (1999) Surface plasmon resonance sensors: review. Sensors and Actuators B 54: 3–15. DOI: https://doi.org/10.1016/S0925-4005(98)00321-9

[72]. Liu Yun, Liu Qiang, Chen Shimeng, Cheng Fang, Wang Hanqi, and Peng Wei (2015) Surface Plasmon Resonance Biosensor Based on Smart Phone Platforms. Sci Rep 5: 12864. DOI: https://doi.org/10.1038/srep12864

[73]. Kysylychyn Dmytro, Piatnytsia Volodymyr, and Lozovski Valeri (2013) Electrodynamic interaction between a nanoparticle and the surface of a solid. Phys Rev E 88: 052403. DOI: 10.1103/PhysRevE.88.052403